Northumbria Research Link

Mechanical Bending Induced Catalytic Activity Enhancement of Monolayer 1T'-MoS$_2$ for Hydrogen Evolution Reaction

Wenwu Shi,[1] Zhiguo Wang,[1*] Yong Qing Fu[2*]

1 *School of Physical Electronics, Center for Public Security Information and Equipment Integration Technology, University of Electronic Science and Technology of China, Chengdu, 610054, P.R. China*
2 *Faculty of Engineering and Environment, University of Northumbria, Newcastle upon Tyne, NE1 8ST, UK*

*Corresponding author. E-mail: zgwang@uestc.edu.cn(ZW); richard.fu@northumbria.ac.uk(YF)

Abstract:

In this paper, mechanisms behind enhancement of catalytic activity of MoS$_2$ mono-layer for hydrogen evolution reaction (HER) by mechanically applying mechanically bending strain was were investigated using density functional theory. Results showed that with the increase of bending strains, the Gibbs free energy for hydrogen adsorption on the MoS$_2$ mono-layer was decreased from 0.18 to -0.04 eV and to 0.13 eV for the bend strains applied along the zigzag and armchair directions, respectively. The mechanism for improvement of the enhanced catalytic activity comes from the changes of density of electronic states near the Fermi energy level, which are induced by the changes of the Mo-S and Mo-Mo bonds upon bending. This report provides a new design methodology to improve the catalytic activity of catalysts based on two-dimensional transition metal dichalcogenides based catalysts through a simple mechanical bending.

Keywords: Hydrogen evolution reaction, transition metal dichalcogenides, mechanical bending, density functional theory

1. Introduction

The current world-wide energy crisis ~~world-wide~~ is complicated by the limited supply of fossil fuel and environmental concerns associated with emission of carbon dioxide from burning fossil fuels. Therefore, it is urgent to explore large-scale non-fossil alternatives of clean energy sources. Hydrogen, one of the most abundant elements in the universe, is considered to be one of the most promising alternatives to carbon-based fuels (Dunn, 2002). However, hydrogen does not naturally exist in large quantities or high concentrations, and must be produced from the other compounds, including fossil fuels (Xia, Zhao, Ye, & Wang, 2014). Water splitting is one of the most promising methods for mass production of hydrogen (Deng et al., 2014; Jaramillo, Jørgensen, et al., 2007; Laursen, Kegnæs, Dahl, & Chorkendorff, 2012; Y. Li et al., 2011), and the key component in the electrochemical ~~reduction~~ splitting of water is the efficient catalyst for hydrogen evolution reaction (HER) (H. Pan, 2014). ~~Platinum group noble~~ Noble metals such as platinum are well-known superb catalysts for electrolysis of water, however, their scarcity and high cost limit their wide-spread usages to produce hydrogen (Fang & Liu, 2009; Jiang, Myer, Tellefsen, & Pau, 2009; Kye et al., 2013; Skúlason et al., 2010; J. Zhang, Sasaki, Sutter, & Adzic, 2007; T. Zhang & Anderson, 2007). Therefore, many researchers have tried to search and ~~design~~ synthesize new catalysts composed of cheaper materials, or ~~using~~ to use micro- or nano-structured compounds and multi-elements-alloys (An,

2

Fan, Luo, & Lau, 2017; Chen et al., 2016; C. Tsai, Abild-Pedersen, & Norskov, 2014) for electrochemical HER.

Monolayer transition metal disulfides (such as MoS_2) are considered to be a promising electro-catalyst for HER. The transition metal disulfides show several types of crystal structures, including 2H (hexagonal structure), 1T (octahedral structure) and 1T' (distorted octahedral structure) structures (Qian, Liu, Fu, & Li, 2014; Song, Park, & Choi, 2015; Wypych & Schollhorn, 1992), strongly depending strongly on the arrangement of S and transition metal atoms. $2H-MoS_2$ is semiconducting in nature, whereas the 1T-MoS_2 is metallic-like (Damien Voiry, Maryam Salehi, et al., 2013). $2H-MoS_2$ shows a poor catalytic activity and the active sites are only located at Mo-terminated edge sites (Jaramillo, Jorgensen, et al., 2007). The basal planes of the $2H-MoS_2$ are inert for HER. Although $1T-MoS_2$ shows a better catalytic performance for the HER, it is metastable at room temperature (Capitani et al., 2013; Enyashin et al., 2011; T. Hu, R. Li, & J. Dong, 2013; Lin, Dumcenco, Huang, & Suenaga, 2014; Damien Voiry, Maryam Salehi, et al., 2013). $1T-MoS_2$ phase will transfer into $1T'-MoS_2$ phase during HER process (G. Gao et al., 2015), and this phase transformation can be used to enhance the catalytic activity of the MoS_2 (G. Gao et al., 2015). Doping is a commonly used method to improve the catalytic performance of MoS_2 (Deng et al., 2015; B. B. Li et al., 2015; Charlie Tsai, Chan, Nørskov, & Abild-Pedersen, 2015a; Wang et al., 2015), however, doping elements are often noble metals which need expensive synthesis equipment such as plasma device synthesis or a well-controlled chemical vapor deposition process (Deng et al., 2015; B. B. Li et al., 2015; Charlie Tsai et al., 2015a; Wang et al., 2015).

3

Mechanical bending strain has frequently been used to modulate the bandgap of MoS_2 (Lloyd et al., 2016) and gas adsorption on MoS_2 (Sahoo, Wang, Zhang, Shimada, & Kitamura, 2016). It can cause changes of the bond lengths and ~~will~~ significantly affect the density of electronic states near the Fermi energy level, thus can ~~could~~ enhance the catalytic performance of MoS_2. Therefore, in this work, we investigate~~d~~ the catalytic activity of basal plane of the 1T'-MoS_2 tuned by applied mechanical strain using density functional theory (DFT) calculations. Calculated results show that the mechanical strain can dramatically affect the HER. The catalytic activity of 1T'-MoS_2 for HER can be enhanced by applying the mechanical strain. This study provides a rational design methodology to improve catalytic activity of catalysts based on two-dimensional transition metal disulfides ~~based catalysts~~.

2. Computational details

The catalytic behaviors of 1T'-MoS_2 were studied using spin-polarized DFT as implemented in the Vienna ab initio simulation package (VASP) code (Kresse & Furthmüller, 1996; Tong, Zhang, Zhang, Liu, & Liu, 2014). The projector-augmented wave (PAW) method and the generalized gradient approximation (GGA) with the Perdew-Burk-Ernzerhof (PBE) functional (Perdew, Burke, & Ernzerhof, 1996) were used to describe electron-ion interactions and exchange-correlation, respectively. Plane-wave basis sets with an energy cutoff of 520 eV were used.

A 6×6 supercell was used to model the monolayer 1T'-MoS_2, which include~~s~~d 36 Mo and 72 S atoms~~, respectively~~. k-point mesh (2×2×1) of Monkhorst-Pack was used for the integration

of Brillouin zone (Pack & Monkhorst, 1977). Two mechanical bending conditions were considered, i.e. along zigzag and armchair directions. In order to use the periodic boundary conditions, we used the rippled supercells as shown in Figs. 1a and 1b to represent mechanical bending applied along zigzag and armchair directions, respectively. The supercells contain 162 and 192 atoms for the zigzag and armchair mechanical bending, respectively. The mechanical strain was realized by bending the MoS_2 monolayer as shown in Fig. ~~2~~1. The mechanical strain was quantified ~~by~~ using a simple kinetic equation: $\varepsilon = T/2R$, where T indicates the peak (or valley) thickness and ~~the~~ R indicates the mechanical bending radius of the monolayer MoS_2 (Lee, Jang, Han, & Baik, 2014). Different mechanical strains can be applied with different values of bending radius.

Since the 1T'-MoS_2 is composed of three atomistic layers, the outside layer is subjected to tensile strain, whereas the inside layer is subjected to compressive strain. The previous study show~~s~~ed that the tensile strain ~~is~~ was beneficial for improvement of the catalytic activity [40]. We only considered the adsorption of H at the outside layer when the mechanical bending was applied on the 1T'-MoS_2, as shown in Fig. 1. During the simulation, all atoms were allowed to relax freely using the conjugate gradient approximation (CG) until the force on each atom was less than 0.02 eV/Å. In order to avoid the periodic image interactions between the bending structure of 1T'-MoS_2 monolayers, the distance between layers was separated by 30 Å vacuum space.

The Gibbs free energy ΔG_H was calculated using equation (1), which ~~can~~ was used to compare ~~characterize~~ the HER activity of materials.

5

$$\Delta G_{\mathrm{H}} = \Delta E_{\mathrm{H}} + \Delta E_{\mathrm{ZPE}} - T\Delta S_{\mathrm{H}} \tag{1}$$

where ΔS_{H} and ΔE_{ZPE} are the entropy difference and zero-point energy difference between the adsorbed state and the gas phase of hydrogen, respectively. ΔS_{H} is usually approximated as $\Delta S_{\mathrm{H}} = \frac{1}{2} S_{\mathrm{H_2}}$, where the $S_{\mathrm{H_2}}$ is entropy of gas phase hydrogen at 300 K with an atmospheric pressure of 1 bar. ΔE_{H} is the hydrogen chemisorption energy, which can be calculated using equation (2).

$$\Delta E_{\mathrm{H}} = E(\mathrm{MS_2 + H}) - E(\mathrm{MS_2}) - \frac{1}{2} E(\mathrm{H_2}) \tag{2}$$

where $E(\mathrm{MS_2 + H})$ and $E(\mathrm{MS_2})$ are the total energy of MoS_2 with and without hydrogen adsorption, respectively. $E(\mathrm{H_2})$ is the total energy of a molecule hydrogen under the gas phase. The value of $\Delta E_{\mathrm{ZPE}} - T\Delta S_{\mathrm{H}}$ ~~is~~ was reported to be about 0.24 eV (Nørskov et al., 2005; H. Pan, 2016; Hui Pan, Feng, & Lin, 2010; Damien Voiry, Hisato Yamaguchi, et al., 2013). Therefore, the Gibbs free energy of hydrogen adsorption ~~can be~~was calculated using $\Delta G_{\mathrm{H}} = \Delta E_{\mathrm{H}} + 0.24$.

3. Results and discussion

The calculated lattice constants are a=3.192 Å, b=6.542 Å for 1T'-MoS$_2$, which are close to previously reported calculated values of a=3.175 Å, b=6.543 Å for the 1T'-MoS$_2$ (Ting Hu, Rui Li, & Jinming Dong, 2013). Side-view and top-view of the two dominant adsorption sites for the H atoms are shown in Fig. 2, and they are the preferable adsorption sites for hydrogen reported in many references (Chou et al., 2015; G. Gao et al., 2015; H. Pan, 2014; Putungan, Lin, & Kuo, 2015).

The HER generally proceeds via two key steps. The first step is Volmer step in which the H atoms are bound to the catalyst site (*) ($H^+ + e^- + * = H^*$). Jiao et al. (M.-R. Gao et al., 2015) have proven that the Volmer step is the rate-determining of HER on the MoS_2. The second step is the Heyrovsky (Skulason et al., 2007) or Tafel step (Skúlason et al., 2010), in which molecular hydrogen is released and leaves the catalyst site ($H^* + H^+ + e^- = H_2 + *$ or $2H^* = H_2 + 2*$). Tang ~~et al~~and Jiang~~.~~ (Tang & Jiang, 2016) ~~have~~ reported that the Heyrovsky reaction (activation energy ~0.62 eV) has a relatively ~~much~~ lower barrier than the Tafel reaction (activation energy ~1.07 eV) for the hydrogen desorption process, hence, the HER occurs mainly via the Volmer-Heyrovsky mechanism on 1T-MoS_2 monolayer. The Gibbs free energy (ΔG_H) of H atom adsorbed on the materials is often used to characterize the HER activity of materials. According to thermodynamics, the materials will show their best catalytic activity with $\Delta G_H = 0$ (Greeley, Jaramillo, Bonde, Chorkendorff, & Nørskov, 2006; Jiao, Zheng, Jaroniec, & Qiao, 2015; Schmickler & Trasatti, 2006). If $\Delta G_H > 0$, the hydrogen will be difficult to bind with the catalyst, whereas if $\Delta G_H < 0$, the hydrogen is strongly adsorbed on the catalyst which can hinder release of the molecular hydrogen.

There are two types of S atoms in 1T'-MoS_2 monolayer, i.e. Sc and St atoms, which have shorter and longer Mo-S bonds, respectively. Sc and St atoms can be assumed equivalent to S atoms subjected to compressive and tensile stresses, respectively (Chou et al., 2015; G. Gao et al., 2015; H. Pan, 2014; Putungan et al., 2015; Charlie Tsai, Chan, Nørskov, & Abild-Pedersen, 2015b). The Gibbs free energies are 0.82 and 0.18 eV for H adsorption at the Sc and St sites on 1T'-MoS_2, respectively, which agree with previously reported calculation results of 0.82 eV and

Commented [RF17]: Using "Greeley et al", "Jiao et al".. not putting all author names..

Commented [RF18]: Using "et al"..

0.19 eV (Putungan et al., 2015; D. Voiry et al., 2013). Based on the above results, the St site is more catalytic active than the Sc site for H adsorption on the basal plane. However, the Gibbs free energy for the Sc site is still higher than 0.19 eV. Whereas the Gibbs free energy for H adsorption on the 1T'-MoS$_2$ monolayer is much smaller than that on 2H-MoS$_2$ monolayer with ΔG_H=2.16 eV [14], indicating the 1T'-MoS$_2$ monolayer is more catalytic activate which agrees with the experimental observations (Damien Voiry, Maryam Salehi, et al., 2013).

To ~~get an insight into~~investigate the mechanism of improved catalytic activity, we analyzed the changes of bond evolution during bending of MoS$_2$. There are two types of Mo-S bonds for each S atom as shown in Fig. 2. Symbols of bt1 and bt2 denote the Mo-S bonds for the S atom located at the St sites, and symbols of bc1 and bc2 denote those for S atoms at the Sc sites. Results show that bt1=2.48 and bt2=2.52 Å for S at St sites, and bc1=2.39 and bc2=2.43 Å for S at Sc sites. The bonds are longer for S at St sites than those at the Sc sites. Comparing the different catalytic activities of Sc and St atoms, the S atoms subjected to tensile strain could generate an improved catalytic activity.

The adsorption of H on 1T'-MoS$_2$ with different bending strains was investigated. Fig. 3a shows the Gibbs free energy of hydrogen adsorbed at the Sc and St sites as a function of bending strain. The Gibbs free energy decreases from 0.82 to 0.43 eV as the bending strain is increased from 0 to 9.89% when the hydrogen atom is adsorbed at Sc site and the 1T'-MoS$_2$ is subjected to a bending along the armchair direction. At the same bending strain, the Gibbs free energy decreases from 0.18 to 0.12 eV when the hydrogen atom is adsorbed at St site on the 1T'-MoS$_2$. Clearly the bending strain has an obvious influence when the H atom is adsorbed at the Sc site

on 1T'-MoS$_2$ when the bending is along the zigzag direction. The obtained Gibbs free energy is decreased from 0.18 to -0.04 eV, which is very close to the best value of $\Delta G_\text{H} = 0$.

Figs. 3b and 3c show the lengths of Mo-S bonds as a function of bending strain as the bending is applied along the zigzag and armchair directions, respectively. The bond lengths increase with the increase of bending strain. For example, ~~as~~ when the bending strain is increased from 0.0% to 9.55%, the values of b1t and bt2 are increased from 2.48 and 2.52 Å to 2.52 and 2.54 Å, respectively, when the bending is applied along the zigzag direction.

With the change of Mo-S bond, the distance between adjacent metal atoms also changes. There are two types of Mo-Mo bonds in 1T'-MoS$_2$ as shown in Fig. 2, which denoted as b1 and b2, respectively. The calculated Mo-Mo distances are 2.78 and 3.19 Å for the 1T'-MoS$_2$ for b1 and b2 which agree well with previously reported values of 2.77 and 3.18 Å (Chou et al., 2015). As shown in Fig. 3d, the two different Mo-Mo bond lengths all increase with the increase of bending strain. As the bending strain is increased to 9.55%, the value of b1 is increased from 2.78 to 2.82 and that of b2 from 3.19 to 3.22 Å when the bending is applied along the zigzag direction.

From the above results, clearly the improvement of the catalytic activity shows a strong dependence ~~on~~ of the Mo-S and Mo-Mo bonds on the bending strain ~~on the Mo-S and Mo-Mo bonds~~. The changes of the Mo-S and Mo-Mo bond lengths can significantly affect the density of electronic states near the Fermi energy level of the MoS$_2$, thus affect its electrochemical activities.

Commented [RF19]: Checking which is depend on which?

9

Fig. 4 shows partial density of states (PDOS) for pristine 1T'-MoS$_2$ (Fig. 4a) and those 1T'-MoS$_2$ bent along zigzag direction with a bending strain of 9.55% (Fig. 4b) and those of 1T'-MoS$_2$ bent along armchair direction with a bending strain of 9.89% (Fig. 4c). The pristine 1T'-MoS$_2$ shows a non-metallic behavior with a bandgap of 0.3 eV, which is close to the previously reported value of 0.375 eV (Ting Hu et al., 2013). The valence bands and conduction bands near the Fermi energy level mainly come from the 3p orbitals of S atoms and 4d orbitals of Mo atoms. Upon bending, the hybridization between Mo d-orbitals and S p-orbitals increases, and accordingly the valence band and conduction band of 1T'-MoS$_2$ move upward and downward in energy values, respectively. The increased density of states near the Fermi energy level will facilitate the supply of electrons to the adsorption sites of 1T'-MoS$_2$, thus resulting in the improvement of its catalytic activity.

The Gibbs free energy of hydrogen adsorption on the mechanically bent MoS$_2$ is close to that of hydrogen adsorbed on the Mo-edge of the MoS$_2$ (C. Tsai et al., 2014; Wang et al., 2015), noble metals (Skúlason et al., 2010) and composite nano-materials (C. Tsai et al., 2014). The HER activity of MoS$_2$ monolayer can be enhanced by the mechanical bending. Therefore, we can conclude that mechanical bending can be used as an efficient way for the improvement of HER activity of two-dimensional transition metal dichalcogenides. The bending strain can be realized by deposition of 1T'-MoS$_2$ on flexible substrates, such as polymethyl methacrylate to apply controllable and reproducible strains on the 1T'-MoS$_2$ (He, Poole, Mak, & Shan, 2013).

4. Conclusion

In summary, we have studied the catalytic behavior of 1T'-MoS$_2$ under mechanical bending using DFT. Gibbs free energy, a key parameter to describe the HER activity of the materials, was calculated for hydrogen adsorbed on pristine and bent 1T'-MoS$_2$, with different bending strains. Gibbs free energy ~~is~~ was decreased from 0.18 to -0.04 eV with the increase of bending strain from 0 to 9.55% as the bending applied along the zigzag direction. We concluded that the improvement of the catalytic activity comes from the density of electronic states near the Fermi energy level, which is induced by the change of the Mo-S and Mo-Mo bonds. This report provides a new methodology to improve the catalytic activity of catalysts based on two-dimensional transition metal dichalcogenides ~~based catalysts~~ through simple mechanical bending.

Compliance with Ethical Standards:

Conflict of Interest: The authors declare that they have no conflict of interest.

References

An YR, Fan XL, Luo ZF, Lau WM (2017) Nanopolygons of Monolayer MS2: Best Morphology and Size for HER Catalysis. Nano Letters, 17:368-376

Capitani F, Höppner M, Joseph B, Malavasi L, Artioli GA, Baldassarre L, et al. (2013) Combined experimental and computational study of the pressure dependence of the vibrational spectrum of solid picene C 22 H 14. Physical Review B Condensed Matter, 88:4745-4751

Chen X, Wang Z, Qiu Y, Zhang J, Liu G, Zheng W, et al. (2016) Controlled growth of vertical 3D MoS2(1−x)Se2x nanosheets for an efficient and stable hydrogen evolution reaction. J. Mater. Chem. A, 4:18060-18066

Chou SS, Sai N, Lu P, Coker EN, Liu S, Artyushkova K, et al. (2015) Understanding catalysis in a multiphasic two-dimensional transition metal dichalcogenide. Nat Commun, 6:8311

Deng J, Li H, Xiao J, Tu Y, Deng D, Yang H, et al. (2015) Triggering the electrocatalytic hydrogen evolution activity of the inert two-dimensional MoS2surface via single-atom metal doping. Energy Environ. Sci., 8:1594-1601

Deng J, Yuan W, Ren P, Wang Y, Deng D, Zhang Z, et al. (2014) High-performance hydrogen evolution electrocatalysis by layer-controlled MoS2 nanosheets. RSC Advances, 4:34733-34738

Dunn S (2002) Hydrogen futures: toward a sustainable energy system. International Journal of Hydrogen Energy, 27:235-264

Enyashin AN, Yadgarov L, Houben L, Popov I, Weidenbach M, Tenne R, et al. (2011) New route for stabilization of 1T-WS2 and MoS2 phases. Journal of Physical Chemistry C, 115:24586-24591

Fang Y-H, Liu Z-P (2009) Surface Phase Diagram and Oxygen Coupling Kinetics on Flat and Stepped Pt Surfaces under Electrochemical Potentials. The Journal of Physical Chemistry C, 113:9765-9772

Gao G, Jiao Y, Ma F, Jiao Y, Waclawik E, Du A (2015) Charge Mediated Semiconducting-to-Metallic Phase Transition in Molybdenum Disulfide Monolayer and Hydrogen Evolution Reaction in New 1T′ Phase. The Journal of Physical Chemistry C, 119:13124-13128

Gao M-R, Liang J-X, Zheng Y-R, Xu Y-F, Jiang J, Gao Q, et al. (2015) An efficient molybdenum disulfide/cobalt diselenide hybrid catalyst for electrochemical hydrogen generation. Nat Commun, 6:

Greeley J, Jaramillo TF, Bonde J, Chorkendorff IB, Nørskov JK (2006) Computational high-throughput screening of electrocatalytic materials for hydrogen evolution. Nat Mater, 5:909-913

He K, Poole C, Mak KF, Shan J (2013) Experimental Demonstration of Continuous Electronic Structure Tuning via Strain in Atomically Thin MoS2. Nano Letters, 13:2931-2936

Hu T, Li R, Dong J (2013) A new (2×1) dimerized structure of monolayer 1T-molybdenum disulfide, studied from first principles calculations. The Journal of Chemical Physics, 139:174702

Hu T, Li R, Dong J (2013) A new (2×1) dimerized structure of monolayer 1T-molybdenum disulfide, studied from first principles calculations. Journal of Chemical Physics, 139:174702-174702-174707

Jaramillo TF, Jørgensen KP, Bonde J, Nielsen JH, Horch S, Chorkendorff I (2007) Identification of active edge sites for electrochemical H2 evolution from MoS2 nanocatalysts. Science, 317:100-102

Jaramillo TF, Jorgensen KP, Bonde J, Nielsen JH, Horch S, Chorkendorff I (2007) Identification of active edge sites for electrochemical H2 evolution from MoS2 nanocatalysts. Science, 317:100-102

Jiang L, Myer B, Tellefsen K, Pau S (2009) A planar microfabricated electrolyzer for hydrogen and oxygen generation. Journal of Power Sources, 188:256-260

Jiao Y, Zheng Y, Jaroniec M, Qiao SZ (2015) Design of electrocatalysts for oxygen- and hydrogen-involving energy conversion reactions. Chemical Society Reviews, 44:2060-2086

Kresse G, Furthmüller J (1996) Efficient iterative schemes for \textit{ab initio} total-energy calculations using a plane-wave basis set. Physical Review B, 54:11169-11186

Kye J, Shin M, Lim B, Jang J-W, Oh I, Hwang S (2013) Platinum Monolayer Electrocatalyst on Gold Nanostructures on Silicon for Photoelectrochemical Hydrogen Evolution. Acs Nano, 7:6017-6023

Laursen AB, Kegnæs S, Dahl S, Chorkendorff I (2012) Molybdenum sulfides—efficient and viable materials for electro - and photoelectrocatalytic hydrogen evolution. Energy & Environmental Science, 5:5577-5591

Lee JH, Jang WS, Han SW, Baik HK (2014) Efficient hydrogen evolution by mechanically strained MoS2 nanosheets. Langmuir, 30:9866-9873

Li BB, Qiao SZ, Zheng XR, Yang XJ, Cui ZD, Zhu SL, et al. (2015) Pd coated MoS2 nanoflowers for highly efficient hydrogen evolution reaction under irradiation. Journal of Power Sources, 284:68-76

Li Y, Wang H, Xie L, Liang Y, Hong G, Dai H (2011) MoS2 Nanoparticles Grown on Graphene: An Advanced Catalyst for the Hydrogen Evolution Reaction. Journal of the American Chemical Society, 133:7296-7299

Lin YC, Dumcenco DO, Huang YS, Suenaga K (2014) Atomic mechanism of the semiconducting-to-metallic phase transition in single-layered MoS2. Nature Nanotechnology, 9:391-396

Lloyd D, Liu X, Christopher JW, Cantley L, Wadehra A, Kim BL, et al. (2016) Band Gap Engineering with Ultralarge Biaxial Strains in Suspended Monolayer MoS2. Nano Letters, 16:5836-5841

Nørskov JK, Bligaard T, Logadottir A, Kitchin JR, Chen JG, Pandelov S, et al. (2005) Trends in the Exchange Current for Hydrogen Evolution. Journal of the Electrochemical Society, 152:J23

Pack JD, Monkhorst HJ (1977) "Special points for Brillouin-zone integrations"\char22{}a reply. Physical Review B, 16:1748-1749

Pan H (2014) Metal dichalcogenides monolayers: novel catalysts for electrochemical hydrogen production. Sci Rep, 4:5348

Pan H (2016) Tension-Enhanced Hydrogen Evolution Reaction on Vanadium Disulfide Monolayer. Nanoscale Res Lett, 11:113

Pan H, Feng YP, Lin J (2010) Enhancement of Hydrogen Evolution on Tungsten Doped Platinum. Journal of Computational and Theoretical Nanoscience, 7:547-551

Perdew JP, Burke K, Ernzerhof M (1996) Erratum: Generalized Gradient Approximation Made Simple [Phys. Rev. Lett. 77, 3865 (1996)]. Phys.rev.lett1396

Putungan DB, Lin SH, Kuo JL (2015) A first-principles examination of conducting monolayer 1T'-MX(2) (M = Mo, W; X = S, Se, Te): promising catalysts for hydrogen evolution reaction and its enhancement by strain. Phys Chem Chem Phys, 17:21702-21708

Qian X, Liu J, Fu L, Li J (2014) Quantum spin Hall effect in two-dimensional transition metal dichalcogenides. Science, 346:1344-1347

Sahoo MPK, Wang J, Zhang Y, Shimada T, Kitamura T (2016) Modulation of Gas Adsorption and Magnetic Properties of Monolayer-MoS2 by Antisite Defect and Strain. The Journal of Physical Chemistry C, 120:14113-14121

Schmickler W, Trasatti S (2006) Comment on "Trends in the Exchange Current for Hydrogen Evolution" [J. Electrochem. Soc., 152, J23 (2005)]. Journal of the Electrochemical Society, 153:L31

Skúlason E, Tripkovic V, Björketun ME, Gudmundsdóttir S, Karlberg G, Rossmeisl J, et al. (2010) Modeling the Electrochemical Hydrogen Oxidation and Evolution Reactions on the Basis of Density Functional Theory Calculations. The Journal of Physical Chemistry C, 114:18182-18197

Skulason E, Karlberg GS, Rossmeisl J, Bligaard T, Greeley J, Jonsson H, et al. (2007) Density functional theory calculations for the hydrogen evolution reaction in an electrochemical double layer on the Pt(111) electrode. Physical Chemistry Chemical Physics, 9:3241-3250

Song I, Park CChoi HC (2015) Synthesis and properties of molybdenum disulphide: from bulk to atomic layers. RSC Advances, 5:7495-7514

Tang Q, Jiang D-e (2016) Mechanism of Hydrogen Evolution Reaction on 1T-MoS2from First Principles. ACS Catalysis, 6:4953-4961

Tong CJ, Zhang H, Zhang YN, Liu H, Liu LM (2014) New manifold two-dimensional single-layer structures of zinc-blende compounds. J.mater.chem.a, 2:17971-17978

Tsai C, Abild-Pedersen F, Norskov JK (2014) Tuning the MoS2 edge-site activity for hydrogen evolution via support interactions. Nano Letters, 14:1381-1387

Tsai C, Chan K, Nørskov J, KAbild-Pedersen F (2015a) Rational design of MoS2catalysts: tuning the structure and activity via transition metal doping. Catal. Sci. Technol., 5:246-253

Tsai C, Chan K, Nørskov J, KAbild-Pedersen F (2015b) Theoretical insights into the hydrogen evolution activity of layered transition metal dichalcogenides. Surface Science, 640:133-140

Voiry D, Salehi M, Silva R, Fujita T, Chen M, Asefa T, et al. (2013) Conducting MoS2 Nanosheets as Catalysts for Hydrogen Evolution Reaction. Nano Letters, 13:6222-6227

Voiry D, Yamaguchi H, Li J, Silva R, Alves DC, Fujita T, et al. (2013) Enhanced catalytic activity in strained chemically exfoliated WS(2) nanosheets for hydrogen evolution. Nat Mater, 12:850-855

Voiry D, Yamaguchi H, Li J, Silva R, Alves DCB, Fujita T, et al. (2013) Enhanced catalytic activity in strained chemically exfoliated WS2 nanosheets for hydrogen evolution. Nat Mater, 12:850-855

Wang H, Tsai C, Kong D, Chan K, Abild-Pedersen F, Nørskov JK, et al. (2015) Transition-metal doped edge sites in vertically aligned MoS2 catalysts for enhanced hydrogen evolution. Nano Research, 8:566-575

Wypych F, Schollhorn R (1992) 1T-MoS2, a new metallic modification of molybdenum disulfide. Journal of the Chemical Society, Chemical Communications1386-1388

Xia X, Zhao X, Ye W, Wang C (2014) Highly porous Ag-Ag2S/MoS2 with additional active sites synthesized by chemical etching method for enhanced electrocatalytic hydrogen evolution. Electrochimica Acta, 142:173–181

Zhang J, Sasaki K, Sutter E, Adzic RR (2007) Stabilization of Platinum Oxygen-Reduction Electrocatalysts Using Gold Clusters. Science, 315:220-222

Zhang T, Anderson AB (2007) Hydrogen Oxidation and Evolution on Platinum Electrodes in Base: Theoretical Study. The Journal of Physical Chemistry C, 111:8644-8648

Lists of figures captions:

Figure 1 Top- and side-views of atomistic configurations of 1T'-MoS$_2$ bended along (a) zigzag and (b) armchair directions.

Figure 2 Top and side views atomistic configurations of 1T'-MoS$_2$.

Figure 3 (a) Gibbs free energy of hydrogen adsorbed at the Sc and St sites on 1T'-MoS$_2$ as a function of bending curvatures. Bond lengths of Mo-S as a function of bending strain when the bending loaded along the (b) zigzag and (c) armchair directions. And (d) Mo-Mo bond lengths as a function of bending strain.
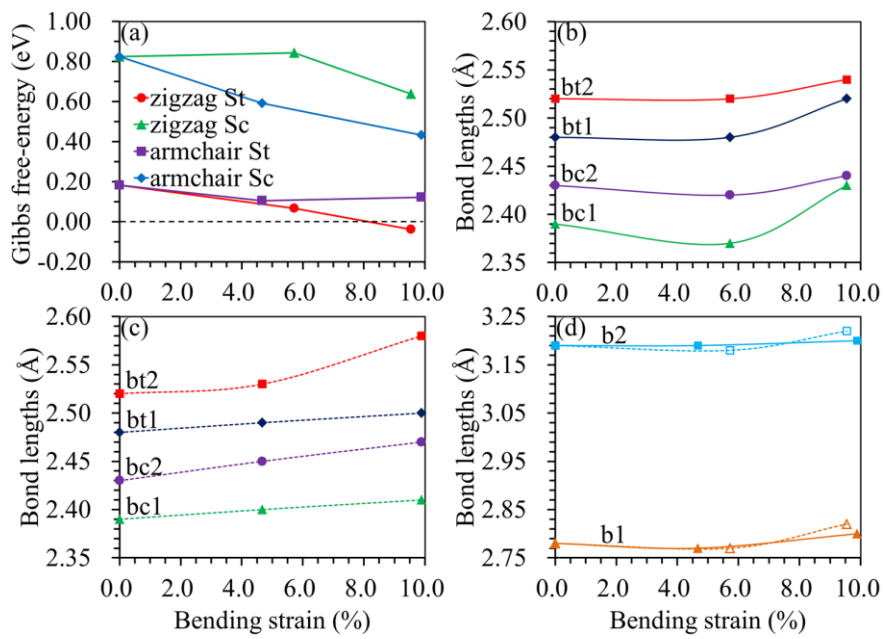
Figure 4 Partial density of states (PDOS) for (a) pristine 1T'-MoS$_2$ and those for bended 1T'-MoS$_2$ along (b) zigzag direction with bending strain of 9.55% and (c) armchair direction with bending strain of 9.89%.
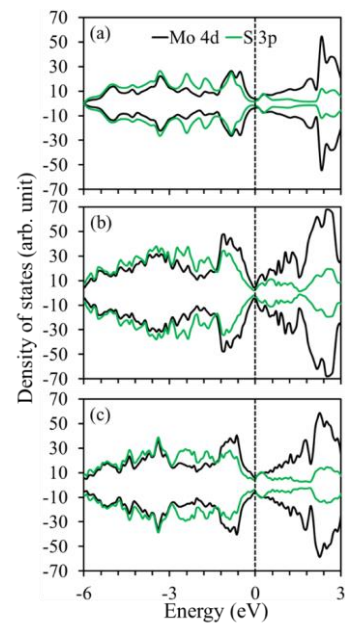
W.W. Shi et al. Figure 1

Top view

Side view

bc1
Sc
bc2
bt1
St
bt2
S
Mo
b1
b2

Sc
St
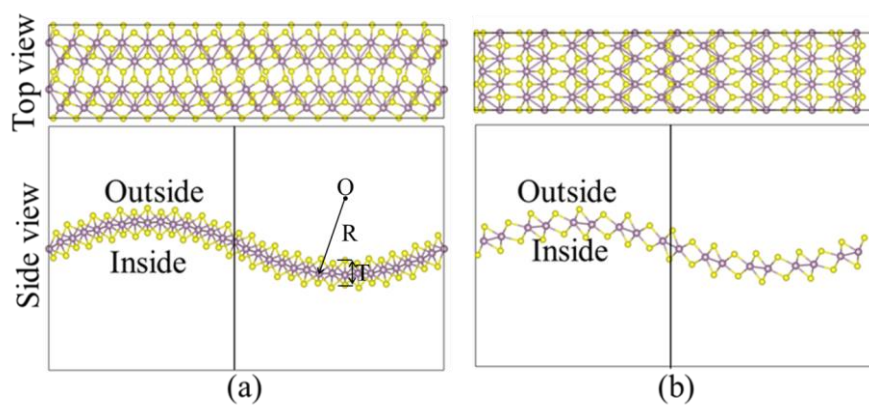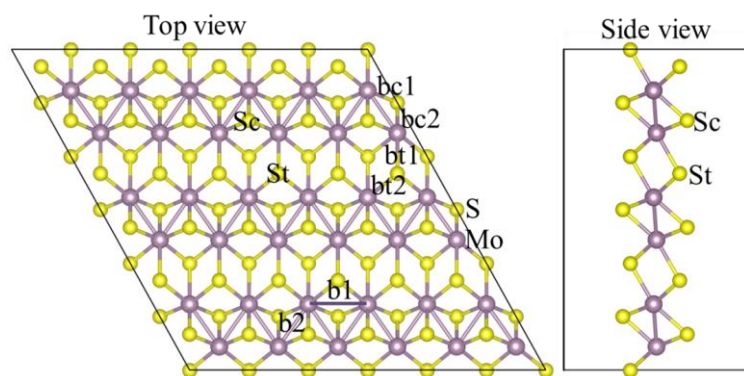
W.W. Shi et al. Figure 2

W.W. Shi et al. Figure 3

W.W. Shi et al. Figure 4

20